Cardiovascular Engineering and Technology, Vol. 6, No. 1, March 2015 *(© 2014)* pp. 8–18
DOI: 10.1007/s13239-014-0205-7

Implicit Partitioned Cardiovascular Fluid–Structure Interaction of the Heart Cycle Using Non-newtonian Fluid Properties and Orthotropic Material Behavior

M.-P. MUEHLHAUSEN,[1] U. JANOSKE,[2] and H. OERTEL JR.[1]

[1]Institute of Fluid Mechanics, Karlsruhe Institute of Technology, KIT, Kaiserstr. 10, building 10.23, 76131 Karlsruhe, Germany; and [2]Chair for Fluid Mechanics, Bergische Universität Wuppertal, Wuppertal, Germany

(Received 28 June 2014; accepted 19 November 2014; published online 17 December 2014)

Associate Editor Ajit P. Yoganathan oversaw the review of this article.

Abstract—Although image-based methods like MRI are well-developed, numerical simulation can help to understand human heart function. This function results from a complex interplay of biochemistry, structural mechanics, and blood flow. The complexity of the entire system often causes one of the three parts to be neglected, which limits the truth to reality of the reduced model. This paper focuses on the interaction of myocardial stress distribution and ventricular blood flow during diastole and systole in comparison to a simulation of the same patient-specific geometry with a given wall movement (Spiegel, Strömungsmechanischer Beitrag zur Planung von Herzoperationen, 2009). The orthotropic constitutive law proposed by Holzapfel *et al.* (Philos. Trans. R. Soc. Lond. Ser. A, 367:3445–3475, 2009) was implemented in a finite element package to model the passive behavior of the myocardium. Then, this law was modified for contraction. *Via* the ALE method, the structural model was coupled to a flow model which incorporates blood rheology and the circulatory system (Oertel, Prandtl—Essentials of Fluid Mechanics, 3rd edn, Springer Science + Business Media, 2010; Oertel et al., Modelling the Human Cardiac Fluid Mechanics, 3rd edn, Universitätsverlag Karlsruhe, 2009). Comparison reveals a good quantitative and qualitative agreement with respect to fluid flow. The motion of the myocardium is consistent with physiological observations. The calculated stresses and the distribution are within the physiological range and appear to be reasonable. The coupled model presented contains many features essential to cardiac function. It is possible to calculate wall stresses as well as the characteristic ventricular fluid flow. Based on the simulations we derive two characteristics to assess the health state quantitatively including solid and fluid mechanical aspects.

Keywords—Blood flow, Orthotropic, Active contraction, KaHMo.

Address correspondence to M.-P. Muehlhausen, Institute of Fluid Mechanics, Karlsruhe Institute of Technology, KIT, Kaiserstr. 10, building 10.23, 76131 Karlsruhe, Germany. Electronic mail: mark-patrick.muehlhausen@kit.edu

INTRODUCTION

Cardiovascular diseases are the most common cause of death in industrialized countries. Besides the mortality, economic losses due to expensive therapies like surgery (Dor procedure, Batista procedure) are important side effects. Hence, considerable research efforts have been undertaken to understand the functionality and interdependencies within the cardiovascular system. Experimental *in vivo* studies would perhaps be the most comprehensive approach to obtain more detailed information. The lack of appropriate measurement techniques and the danger for human patients, however, often prevent these studies from being applied in practice. Although many studies have been carried out on animals like dogs or pigs, these findings cannot generally be applied to humans.

For these reasons, increasing efforts have been dedicated to analytical and numerical modeling of the cardiovascular system in recent decades. In the early beginnings, only a few specialized aspects or domains like heart valves or structural mechanics of the myocardium were modeled separately. First analytical representations of the myocardium were based on thin- or thick-shell assumptions. In the twentieth century, finite element analysis allowed for the formulation of more complex and realistic constitutive equations that also considered anisotropy and inhomogeneity.[7,12–14] Investigation of cardiac blood flow required the description of the endocardium as a function of time. This was achieved using a given generic or MRI-based motion.[15,27]

With increasing knowledge and computational progress, extension and combination of these domains were possible. This led to the so-called fluid–structure interaction which captured the interaction between blood

flow and muscle activity. The huge efforts in this area can generally divided into approaches using ALE[1,23,24,38] or immersed boundary method (IBM)[30,36] for describing the blood flow in the heart. Comprehensive overviews in this field of research can be found in.[5,8,9,11,26,28]

The Karlsruhe Heart Model (KaHMo) is a patient-specific modular framework for the investigation and assessment of the human heart function. An extensive summary about KaHMo can be found in.[25,27 32] KaHMo consists of three branches. KaHMo-MRI uses the given wall motion as a boundary condition for the fluid flow simulation.[33] The wall motion is reconstructed from MRI data. Based on the simulation of the ventricular flow of different healthy, pre and post-surgery patients, we proposed a characteristic to assess the health status. KaHMo-VAD simulates the interaction between the ventricular assist devices and diseased hearts. One of the main topics covered by KaHMo-VAD is blood damage and thrombosis due to artificial shear fields.[29] Within KaHMo-FSI, the given wall motion is replaced by coupling with a structural model of the heart wall. In a first step, we developed a fiber continuum composite model for the myocardium. The main idea of spatial splitting of fiber and matrix follows the procedure of splitting the strain energy potential for different directions.[17]

Although the fiber continuum composite model correctly reproduced the movement of the endocardium, spatial stress distribution still needed improvement due to the model assumptions. The aim of the study reported here was to replace the fiber continuum composite model by a more realistic material description. For this purpose, a spatially varying system of orientations was defined. To capture the passive orthotropic behavior during the diastole, the strain energy function proposed by Holzapfel *et al.*[12] was implemented in the Abaqus finite element package. For simulating the active contraction of the myocardium, we added one term and modified several terms. For validation of the flow field, a coupled simulation was performed and compared to a reference simulation[33] done with the given wall motion. The simulations of a healthy heart covered six heart beats. To guarantee that there is no influence of initial conditions, only the last beat was considered. Based on these simulations we derived a new characteristic called modified non-dimensional pumping work to quantify the health state of the human heart including fluid and solid mechanical aspects.

METHODS

Mechanics and Coupling

The equations describing fluid flow are typically solved in spatially fixed Eulerian coordinates. The structural equations are formulated in a moving Lagrangian frame. In the case of an elastic structure surrounding a fluid domain or being embedded in it, the fluid grid can be described to be deformable. To take the deforming mesh into account, the equations of conservation for the fluid have to be reformulated using the Arbitrary Lagrangian–Eulerian formulation of the Navier–Stokes and continuity equations.

Continuum Mechanics

The deformation gradient $\mathbf{F}$ is the material derivative of motion. Capital letter $\mathbf{X}$ denotes the position in the reference configuration and the small letter $\mathbf{x}$ describes the actual position. As a measure of strain, the right Cauchy Green tensor $\mathbf{C}$ and the Green strain tensor $\mathbf{G}$ are used. The large deformation of the heart muscle requires a geometrical non-linear treatment.

$$F = \frac{\partial \mathbf{x}}{\partial \mathbf{X}} \qquad \mathbf{C} = \mathbf{F}^{\mathbf{T}}\mathbf{F} \qquad \mathbf{G} = \frac{1}{2}(\mathbf{C} - \mathbf{1}).$$

The shear stress within a fluid depends on the symmetric part $\mathbf{D}$ of the velocity gradient $\mathbf{L}$.

Governing Equations

The fluid equations modified for the deformable mesh have to be valid for the endocardium as well as for the atrium and every cell in between. Hence, the velocity $\mathbf{v}$ is defined relative to a grid velocity $\mathbf{v}_g$ which has to fulfill the space conservation law[2,3] and is calculated from the moving boundary and the smoothing mechanism (see "Solution Scheme" section). At the endocardium, the grid is fixed to the heart wall and moves with its velocity $\dot{\mathbf{u}}$ in the direction of displacement $\mathbf{u}$. In this case, the nonlinear convective part of the Navier–Stokes equations vanishes and the equation is written using the Lagrangian frame. Due to the mesh smoothing mechanism, the grid velocity decreases with increasing distance from the moving wall.

$$\nabla \cdot \mathbf{v} = \mathbf{0} \qquad \rho\left(\frac{\partial \mathbf{v}}{\partial t} + (\mathbf{v} - \mathbf{v}_g) \cdot \nabla \mathbf{v}\right) = \sigma_f.$$

Stress Formulation

Blood as well as heart tissue can be assumed to be incompressible. Because of the heart rate (58 beats per minute) and the health state of the considered heart, blood flow is modeled to be laminar. The Cauchy stresses on the right hand side of the momentum conservation law have to be related to the deformation (in case of a solid) or strain rate (in case of a fluid) *via* a constitutive law. The behavior of blood ($\rho = 1055 \frac{\text{kg}}{\text{m}^3}$) is pseudo-plastic, which means that the viscosity decreases with increasing shear rate.

$$\boldsymbol{\sigma}_f = -p\mathbf{I} + 2\mu_{eff}\mathbf{D}.$$

The effective viscosity of blood is a function of the shear rate and described by the Carreau model. The coefficients λ, n, μ_0 and μ_∞, were fitted to experiments by Liepsch *et al.*[21]

$$\mu_{eff} = \mu_\infty + (\mu_0 - \mu_\infty)\left(1 + (\lambda\dot{\gamma})^2\right)^{\frac{n-1}{n}}.$$

The stresses in a structure consisting of a hyperelastic material can be formulated as a function of a strain energy W. J is the determinant of the deformation gradient. For an incompressible material $J = 1$ holds.

$$\boldsymbol{\sigma}_s = -p\mathbf{I} + \frac{1}{J}\mathbf{F}\frac{\partial W}{\partial \mathbf{G}}\mathbf{F}^T.$$

Coupling Technique

The use of the ALE method leads to a set of equations for the structure and the fluid. This set of equations can be solved either in one step for the fluid and structure or separately for the fluid and solid. The former approach is referred to as monolithic, while the second one is called partitioned. The nonlinear material responses of the fluid and solid in the heart need a different and special treatment in the solution process of the system matrices. Assembling of both matrices prevents these treatments and may lead to slow or no convergence. A partitioned approach allows for the use of specialized solvers which can be changed and validated independently. In this case, it is also possible to have different time step sizes for the fluid and the solid. Due to these benefits, a partitioned procedure is chosen.

Coupling Condition

The fluid (index f) and structural (index s) domains (see Figs. 3, 6) are separated from each other by the endocardium (surface-coupled problem). Here, the momentum is exchanged between the fluid and structural solver. The meshes of myocardium and blood are not identical near the interface. For this reason, a flux integral interpolation scheme was used for transferring the momentum.[6] Due to the partitioned coupling approach, the momentum conservation on the interface is formulated with the help of the kinematic and dynamic coupling condition. It says that the position $\mathbf{x}$ of the interface area must be the same in the fluid and the solid. Furthermore, the forces (per area) of the fluid acting on the solid have to be equal to those of the solid acting on the fluid.

$$\mathbf{x}_s = \mathbf{x}_f \qquad \mathbf{t}_s = \sigma_s \cdot \mathbf{n} = -\sigma_f \cdot \mathbf{n} = -\mathbf{t}_f$$

Solution Scheme

The solution scheme defines which and when information is exchanged between the fluid and solid solver. To account for the density ratio of blood and soft tissue and the low stiffness with small strains, an absolute implicit code coupling scheme was developed recently by Krittian *et al.*[18] which is used in this work.

In the beginning of the coupling process, nodes of the finite element mesh on the interface were associated with boundary cells of the fluid mesh. For this purpose, a distance search was conducted. The association was kept constant, because boundary cells are not remeshed during the simulation. The fluid solver calculated the wall stresses acting on the endocardium (Step 1). These wall stresses were integrated over the appropriate boundary cell face area (flux interpolation). The resulting forces—assumed to be in the centers of fluid cell faces—were interpolated at the associated finite element nodes using linear shape functions (Step 2). Due to the loads on the endocardium, the finite element solver calculated mesh deformation and stresses within the myocardium (Step 3). The nodes of the fluid boundary cell faces were projected on the new position of the finite element endocardium using a field interpolation technique in which the new position of the fluid boundary cell face node depends on the position of the surrounding finite element nodes weighted with their distances (Step 4). After the projection, the fluid mesh was smoothed using a spring-based approach. The resulting displacements of the fluid cell divided by the time step size yielded grid velocity. The smoothing approach used reduced the grid velocity with increasing distance from the endocardium. After smoothing, the fluid solver calculated a new solution for inner ventricular blood flow and wall stresses (step 5). The success of coupling was assessed by residuals of load, position, and coupling energy. The load residual resulted from the difference in wall stresses (Steps 1 and 5). The position or better displacement residual resulted from the projection (Step 4). The product of load and displacement residual may be considered to be coupling energy. Steps 1–5 were called coupling iteration and represented one time step. They were repeated with modified positions and forces until the coupling residuals vanished. To ensure that dynamic and kinematic coupling conditions were fulfilled, 5–10 coupling iterations were performed per time step. For the stabilization of the coupling process, a load relaxation mechanism with dynamic relaxation parameter estimation was applied. This means that during coupling iteration of one time step only, several forces were transferred. The dynamic parameter estimation can be done either by coupling residual, inner iteration or Aitken extrapolation.

Software Packages and Hardware

The KaHMo is based on commercial software with extended functionality by user subroutines. For the fluid flow, the Fluent FVM package (Ansys, Release 6) is used. The behavior of the structure is calculated by the FEM code Abaqus (Dassault, Release 6.9). Both codes are coupled *via* MpCCI (Fraunhofer SCAI, Release 3) which is able to perform an explicit coupling by default. Details on the coupling procedure can be found in.[6] All simulations were done on workstations (AMD Phenom II X6 1100T @3,3 GHz, 16 GB RAM).

Fluid and Solid Model

Left Ventricular Heart Model

To validate the material description for the active and passive behavior of the myocardium, a fluid–structure interaction simulation was carried out and compared to a reference simulation with a given wall motion. The endocardium, parts of the atrium, and aorta were reconstructed from ECG-controlled MRI data of the left ventricle of a healthy patient. Additionally, physiological data, such as blood pressure and heart rate, were recorded. As the data were still insufficient, the epicardium was added generically. Segmented MRI data provided closed curves marking the endocardium in horizontal layers. We calculated a centroid of each closed curve. For each horizontal layer, the curve was projected in radial direction to give the position of the epicardium. Doing this, two aspects had to be considered: The thickness of the myocardium was to be within the physiological range (8–12 mm) and the shape of the epicardium was to be sufficiently smooth to reduce geometry-induced excessive stress. The simulation process started at a point in time during the fast filling phase, because this point was considered to be nearly load-free. Residual stresses in the myocardium were not considered in this work.

Discretization and Numerics

The fluid volume was meshed with tetrahedral elements. The mesh within the left ventricle was refined several times to ensure mesh independence. The final mesh consisted of 500000 elements. The flow equations were discretized using the second-order upwind scheme in space and implicit first order in time. The time step size was chosen to be $\Delta t = 0.001$ s, so that a single heart beat was captured with 1000 time steps. The staggered SIMPLE algorithm was used for pressure correction. The structural analysis was also carried out using different mesh densities to guarantee mesh independence. The final mesh consisted of 57,000 linear tetrahedral elements. The myocardium was assumed to be incompressible.

Local Direction Definition

Experimental studies of LeGrice *et al.*[19,20] and Dokos *et al.*[4] revealed that the myocardium has orthotropic properties. This means that the strain–stress response of the heart muscle is different in three distinguished planes. To consider this material behavior, it is necessary to define distinct directions within the heart wall. This can be done using two vectors for the fiber direction $\mathbf{f} = (f_x, f_y, f_z)$ and the sheet direction $\mathbf{s} = (s_x, s_y, s_z)$. The third direction—the sheet-normal direction—results from the cross-product of $\mathbf{f}$ and $\mathbf{s}$. The vectors can be defined using a polar coordinate system and three angles α, β and γ. The angle β and the radius r are used to describe the location of a mesh vertex of the discretized myocardium in horizontal layers (polar coordinate system)

$$
\begin{aligned}
f_x &= \cos(\alpha)\sin\left(\beta+\frac{\pi}{2}\right) + \sin(\alpha)\sin(\gamma)\cos\left(\beta+\frac{\pi}{2}\right)\\
f_y &= \cos(\alpha)\cos\left(\beta+\frac{\pi}{2}\right) - \sin(\alpha)\sin(\gamma)\sin\left(\beta+\frac{\pi}{2}\right)\\
f_z &= \cos(\gamma)\sin(\alpha) \qquad s_x = \cos(\gamma)\sin(\beta)\\
s_y &= \cos(\gamma)\cos(\beta) \qquad s_z = \sin(\gamma).
\end{aligned}
$$

The angle α describes the inclination of the fiber in radial direction (Figs. 1, 2). If α equals 0, the fibers run in concentric circles around the long axis of the heart, so they lie in the horizontal layer. The definition of the sheet direction from the base to apex of the heart needs an additional parameter which has been chosen to be the angle γ. This angle characterizes the gradient of the muscle sheet in radial direction. It is assumed that all sheets start and end perpendicular to the endo- and epicardium. Because of this assumption, γ depends on

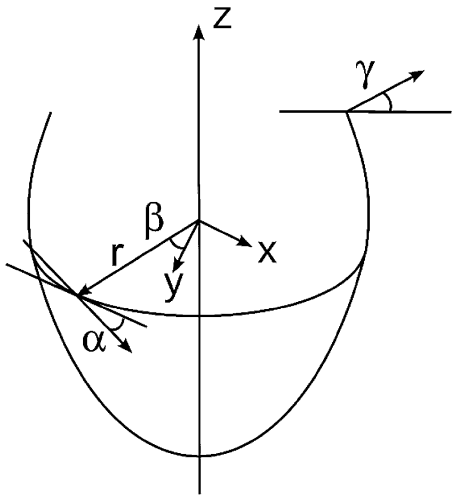

FIGURE 1. Local direction definition.

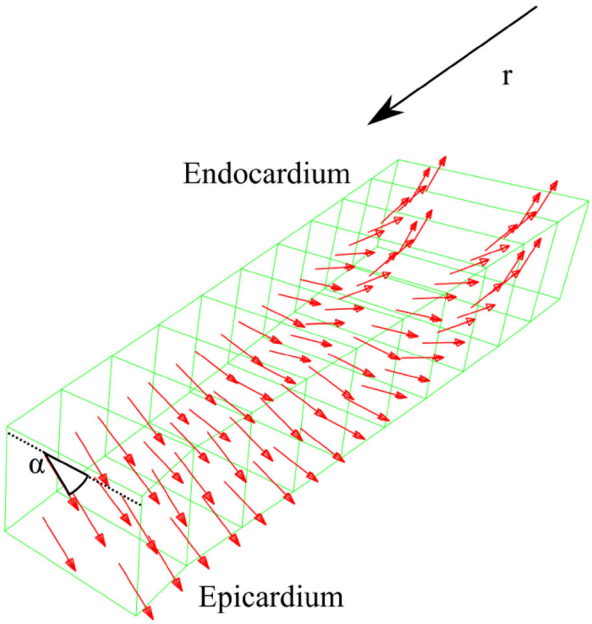

FIGURE 2. Transmural fiber direction.

the normal vectors of the endo- and epicardium. For $\gamma = 0$, the vector $\mathbf{s}$ points in radial direction starting from the long axis and lies in the horizontal layer.

$$\alpha = f(r) \quad \gamma = f(n_{\text{End}}, n_{\text{Epi}}, r)$$

The functions α and γ are assumed to be a fourth-order and a linear function. The constants (exponents) of these functions are fitted manually such that the given motion of the heart known from MRI during the filling phase is represented sufficiently (see "Constitutive Equation" section for details).[22]

Constitutive Equation

Considering experimental studies of the structure and mechanics of the human heart, Holzapfel *et al.*[12] provided a constitutive model for the passive orthotropic stress response of the human heart during the diastole in terms of an energy function. They decomposed the energy function into an isotropic and an anisotropic part. To use this model for a complete heart cycle, it was necessary to modify and expand this equation for the systole condition. For this purpose, we added an additional term W_{active}.

$$W = W_{\text{passive}} + W_{\text{active}} = W_{\text{iso}} + W_{\text{aniso}} + W_{\text{active}}.$$

To fulfill the material objectivity requirement, Holzapfel *et al.*[12] expressed the energy function in terms of invariants of the right Cauchy-Green tensor and the vectors defining fiber and sheet direction. Further information on the derivation of the constitutive model for the passive strain–stress response can be found in Holzapfel *et al.*[12]

$$I_1 = \text{tr}(\mathbf{C}) \quad I_{4\text{f}} = \mathbf{f} \cdot (\mathbf{Cf}) \quad I_{4\text{s}} = \mathbf{s} \cdot (\mathbf{Cs}) \quad I_{8\text{fs}} = \mathbf{f} \cdot (\mathbf{Cs}).$$

The following equation was taken from Holzapfel *et al.*[12] and partially modified to account for contraction via the activation $\text{Akt}(t)$ and the parameters d_i. Goektepe *et al.*[10] used the experimental data of Dokos *et al.*[4] to fit the constants starting with a and b. The muscle fibers were arranged in layers connected by an elastic network. The second term represents the stress caused by an extension of the fibers. The third and fourth terms incorporate the interaction of fiber and sheet direction.

$$\begin{aligned} W = {} & \frac{a}{2b}\exp[b(I_1 - 3)] + \frac{a_{\text{f}}}{2b_{\text{f}}}\left(\exp\left[b_{\text{f}}(I_{4\text{f}} - 1)^2\right] - 1\right) \\ & + \frac{a_{\text{s}}}{2b_{\text{s}}}\left(\exp\left[\frac{b_{\text{s}}}{1 + d_3\text{Akt}(t)^{d_4}}(I_{4\text{s}} - 1)^2\right] - 1\right) \\ & + \frac{a_{\text{fs}}}{2b_{\text{fs}}}\left(\exp\left[\frac{b_{\text{fs}}}{1 + d_3\text{Akt}(t)^{d_4}}(I_{8\text{fs}} - 1)^2\right] - 1\right) \\ & + d_1\text{Akt}(t)I_{4\text{f}}^{d_2}. \end{aligned}$$

The systole is initiated by an electrochemical excitation starting from the sinu-atrial node. For studying the interaction of blood flow and myocardial stress distribution, we used an activation $\text{Akt}(t)$ varying with time. This function is equal to one at the end of the systole and zero in the load-free states before and after the systole. The fifth term of the equation denotes the contraction of the heart. Depending on the activation, the strain energy increases in the direction of the muscle fibers. The muscle sheets rearrange during contraction.[19] This will save energy. Therefore, the cross directions are to result in less resistance, which is represented by the modification of the third and fourth terms. With increasing activation, these terms decrease. To omit the modification results in non-physical high stresses. To leave these terms out leads to a non-physical deformation behavior. For the usage of the model, the parameters d_i, $i = 1, 2, 3, 4$, the orientation of fibers and sheets as well as the functions α and γ have to be determined. This was done in two steps. The first one considers diastole, the second one also systole.

Within the KaHMo-MRI framework, patient-specific MRI data of the time-dependent movement of the endocardium are applied to the fluid flow simulation. The time-dependent pressure variation (needed for boundary condition) in the aorta and the pulmonary vein during a heart cycle results from a circulatory model validated against clinical data. At first, a coupled simulation of the diastole using the validated circulatory model was carried out.[31] The functions α, γ, and the vectors $\mathbf{f}$ and $\mathbf{s}$ in the load-free state for each

FEM mesh node of the myocardium were fitted such that the time-varying pressure in the atrium and pulmonary vein gives the right deformation of the heart. For this purpose, the position of each myocardial mesh node in the load-free state was exported from Abaqus and imported into Matlab at the beginning of the simulation. In Matlab the coordinates were transformed from cartesian into polar coordinates and then into vectors **f** and **s**. The initial shapes for functions α and γ were taken from literature (Streeter *et al.*[34,35]). Afterwards, the vectors for each mesh node were converted back into Abaqus. To fit functions α and γ, the coupled simulation of the diastole was repeated several times until the determined inner ventricular pressure and volume were in good agreement with KaHMo-MRI. For this purpose, the slopes of volume and pressure of two simulations were compared to each other. The constants were slightly modified empirically until a good agreement in volume change was achieved. A good agreement in volume change leads to a good agreement in inner ventricular pressure, because the dynamic pressure part is strongly connected to the derivatives of volume change. To avoid kinks in inner ventricular pressure during the heart cycle, the volume change should be smooth up to the second derivative.

The anatomical structure of the heart is the same in the systole and diastole, such that α and γ can be assumed to be the same in both phases. Secondly, the pressure boundary condition of the circulatory system and the movement of the heart wall are used to fit the parameters d_i during a coupled simulation of the systole. The used constants of the strain energy function are listed in Table 1. Some of the constants for the passive behavior are slightly modified to better fit strains between 0.4 and 0.5.

Boundary Conditions and Heart Valves

The heart is surrounded by the pericardium. The pairing of epicardium and pericardium provides for reduced friction during the large and fast deformation. The present study, however, only considers the fluid–structure interaction between myocardium and blood flow. Momentum between fluid and solid is exchanged at the inner ventricular wall. As the valve plane or the vessels are not part of the interface, their positions are fixed. In our simulation we use a two-dimensional boundary condition on the valve plane. The boundary condition can change as a function of either time or pressure. We found that even if the pressure-driven variant is more realistic, the effect on the ventricular flow field is nearly negligible. The heart is the engine of the circulatory system and, hence, closely connected to it. We used mass flux-dependent pressure boundary conditions at the inlets and outlets of the fluid domain. The actual pressure was calculated during the simulation with a 3-element Windkessel model. The parameters of the model were determined by the procedure implemented by Perschall 2010.[29]

RESULTS

The success of the current modeling approach is evaluated based on solid and fluid mechanics aspects. To the knowledge of the authors, direct measurement of *in vivo* stresses in the heart wall is still impossible. To assess the structural model of the myocardium, we compared coupled simulation to MRI data and physiological observations. Due to the lack of experimental data, the calculated stresses can be evaluated qualitatively only.

Myocardial Deformation and Stress Distribution

Figure 3 shows the volume change during one heart cycle. The good agreement between the calculated inner ventricular volume and the MRI data indicates a correct time-dependent movement of the endocardium. Information about the motion and shape of the epicardium cannot be derived from our data.

During contraction and relaxation, the heart muscle works in a physiological manner. During a systole, the ventricle volume decreases. The ventricle shortens along the long and short axis direction. The thickness of the wall increases because of myocardial incompressibility. Besides these motions, the implemented constitutive model is able to capture the rotation around the long axis. This rotation is due to torque caused by the force of fibers and the radial distance between the position of the fibers and the long axis. The muscle fibers are embedded in sheets producing resistance in the direction perpendicular to the fibers. For this reason, the rotational motion of the heart takes place nearly, but not exactly in fiber direction. In the diastole the pressure difference between the left atrium and ventricle leads to a rapid increase of the ventricle volume. The heart grows in long axis and

TABLE 1. Constants of strain energy function.

a (kPa)	b[−]	a_f (kPa)	b_f (−)	a_s (kPa)	B_s (−)	A_{fs} (kPa)	b_{fs} (−)	d_1 (kPa)	d_2 (−)	d_3 (−)	d_4 (−)
0.000496	7.209	0.015	20.417	0.0015	23.176	0.000662	9.466	1.05	1.1	100000	2

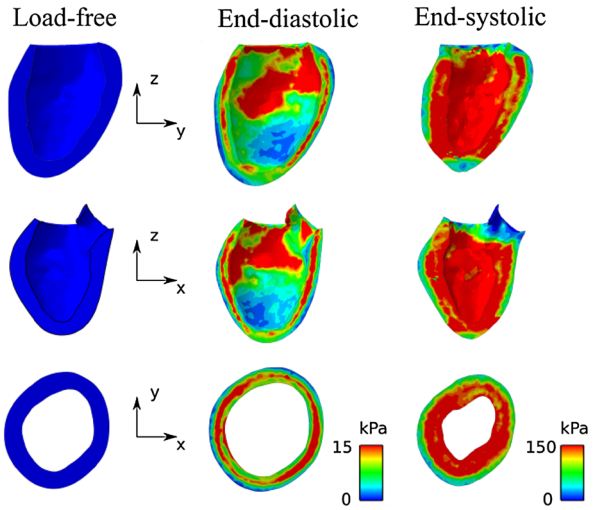

FIGURE 3. Myocardial stress distribution.

radial direction. As in the systole, the same mechanism causes a rotation, but this time, in opposite direction. The calculated motion of the left ventricle seems to be physiological except for one limitation: For the coupled simulation, our current numerical framework requires a positional fixation at the basis of the heart. *In vivo*, long axis shortening happens with an apex nearly fixed and the valve plane doing a vertical motion. This so-called valve plane mechanism is known to support the efficient pumping, but has not yet been implemented. Figure 3 shows the calculated stress distribution in the end systole and end diastole in different planes. During the simulation, the calculated stresses are within the physiological range compared to studies of the stress–strain behavior of single muscle fibers excised specimen from the heart wall.[4,10] The stresses in the diastole are lower than in the systole by nearly one order of magnitude. The highest values are encountered in the mid-wall region, which can be explained by a nearly radial orientation of the muscle fibers. During the diastole, the motion of the myocardium is caused by circulatory pressure. In the end diastole, the wall stresses balance the pressure within the ventricle. In the systole, the muscle fiber contracts and the wall stresses increase, which leads to a pressure increase in the ventricle. When the pressure in the left ventricle exceeds that of the aorta, the aortic valve opens and outflow starts. In the end-systolic state, the left ventricle has its smallest volume and the stresses in the heart wall are maximum. These stresses result nearly solely from balancing the inner ventricular pressure. The physiological observation of sheet rearrangement during systole reduces the work necessary to contract. This is captured by means of the implemented strain energy function. Due to positional restriction at the heart basis, the activation function is blended in vertical direction to avoid non-physiological stresses. The error caused by this blending can be assumed to be negligible. On the one hand, the tissue around the heart valve is stiff and will not be subject to significant displacement. On the other hand, the calculated motion of the heart is in good agreement with MRI data.

Quantitative Assessment of Myocardial Function

The coupled simulation using the newly implemented constitutive equation is compared to a simulation with the given wall motion.[33] For comparison, we use the stroke volume VS, the velocities through valves, the calculated mean viscosity over one heart cycle $\overline{\mu_{\text{eff}}}$ as well as Reynolds and Womersley numbers as defined in Oertel *et al.*[25,27] The heart may be considered a discontinuously working pump. Hence, the work done can be used as a criterion of the health state. This work A_{p} results from the pressure within the ventricle and the inner ventricular volume as well as from the acceleration of the blood. The latter can be neglected, because it is relatively small in comparison to the pressure work for the given heart rate. Additionally, the health state is quantified by the ejection fraction EF and the residence time t_{B20}. The former is the ratio of stroke volume to end-diastolic volume. The latter means the time until only 20% of the "old" blood are still contained in the ventricle. Consequently, the residence time is an indicator of effective mixing and ejection of blood. This capability is strongly connected to the shape of the ventricle and essential for heart function. If blood is at rest (no shearing), it agglomerates and may form a thrombus.

The objective of the KaHMo is to assess the current health state (KaHMo-MRI) and estimate the success of cardiac surgery (KaHMo-FSI). For this reason, it is convenient to define a characteristic quantifying myocardial function. In previous publications, a non-dimensional pumping work O was defined and applied to simulations with a given wall motion based on MRI data.[25,27] As wall motion was given and no model of the heart wall exists, this characteristic only takes into account fluid mechanics aspects. This time, we expand the formulation to capture structural mechanics of the myocardium. Based on dimensional analysis, the two following equations are proposed:

$$O_{\text{S1}} = \frac{A_p \bar{\sigma}_{\text{sys}} t_{\text{B20}}^2}{\overline{\mu_{\text{eff}}^2} V_S} \quad O_{\text{S2}} = \frac{\bar{\sigma}_{\text{sys}} V_{\text{S}}}{A_{\text{p}}}.$$

High values for the already proposed non-dimensional pumping work O suggest a diseased state. O_{S1} is an expansion of O with the end-systolic mean stress in the myocardium. If the thickness of the heart wall

TABLE 2. Quantitative assessment of cardiac function.

	KaHMo-MRI	KaHMo-FSI
Stroke volume (ml)	111.5	113.6
End-diastolic volume (ml)	178.8	180.0
End-systolic volume (ml)	67.4	66.4
Mean mitral velocity (m/s)	0.31	0.32
Mean aortic velocity (m/s)	0.78	0.81
$\overline{\mu_{\text{eff}}}$[g/(ms)]	4.8	4.7
Sys. Reynolds number (–)	3720	3920
Dia. Reynolds number (–)	1675	1744
Sys. Womersley number (–)	25.7	25.9
Dia. Womersley number (–)	29.1	29.3
Ejection fraction (%)	62.3	63.1
Ap (Nm)	1.6	1.7
t_{B20} (s)	1.19	1.19
O (10^6)	3.5	3.7
O_{S1} (10^{14})	–	1.2
O_{S2} (10^6)	–	9.2

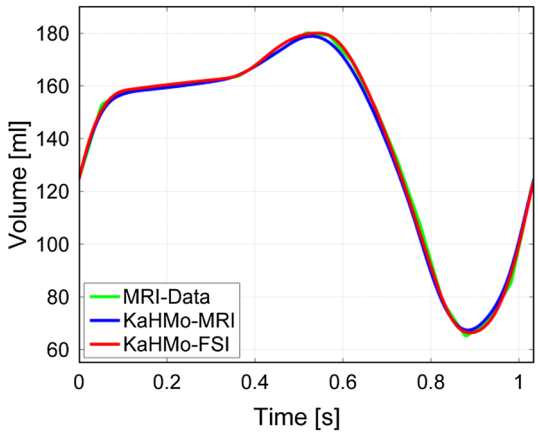

FIGURE 4. Comparison of calculated and measured volume changes during one heart cycle.

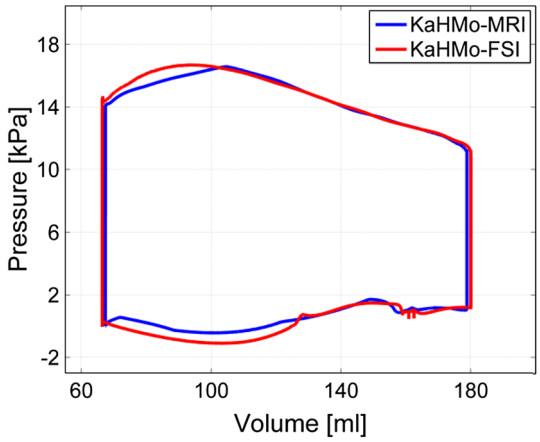

FIGURE 5. Calculated pressure–volume curves during one heart cycle.

decreases due to e.g., heart failure, the mean stress increases. At the same time, the stroke volume will decrease. The second equation O_{S2} reflects the efficiency of the heart. It is the ratio of work done by the heart muscle and the energy increase in the blood. Table 2 shows the calculated values for the parameters mentioned. Figures 4 and 5 compare the volume change and the pressure work for the different modeling approaches. The simulations with a given (KaHMo-MRI) and simulated (KaHMo-FSI) wall motion are in good agreement. Apart from the values for the previously proposed non-dimensional pumping work, Table 1 also lists the values for O_{S1} and O_{S2}. Wall movement based on time-resolved MRI data at best allows for a fluid mechanics-based assessment of the state of health. A structural model of the myocardium offers the chance to predict the success of a modification of the heart wall by surgery. The data presented confirm that KaHMo-FSI is able to capture the actual health state represented by O, which means that the structural model (geometry, fiber orientation, and strain energy function) is sufficiently accurate. A "virtual surgery" on the structural model and a "real surgery" *in vivo* are therefore supposed to produce similar results. As the space- and time-dependent excitation is not simulated, the computational effort is reduced. This aspect is crucial to clinical practice.

Ventricular Blood Flow

Figure 6 compares the evolution of blood flow within the left ventricle at four characteristic times during one heart cycle. The streamlines are colored according to the velocity magnitude and scaled to maximum velocity. The pressure-driven mitral valve opens when the myocardium is completely relaxed and the inner ventricular pressure falls below the pressure of the atrium that initiates the diastole. Due to the high inflow velocity caused by the large pressure difference, a jet with the characteristic ring vortex forms (a). The ring vortex is asymmetric. This can be explained by the different distances between the jet and heart wall on the left and on the right side. At the end of the early filling phase, the pressure difference is small and less blood flows into the ventricle (b). The ring vortex moves towards the apex. Asymmetric growth leads to an additional rotation and an effective mixing in the region near the apex. Subsequently, the ring vortex decays due to viscous effects (c). The small oscillations at the end of the plateau phase just before contraction of the atrium happen over 2–3 time steps and are caused by the two-dimensional time-driven mitral valve (Fig. 5). The inflow velocity is very small and the pressures in the atrium and left ventricle are nearly equal, which causes the mitral valve to close partly. The change of boundary condition (the area where the

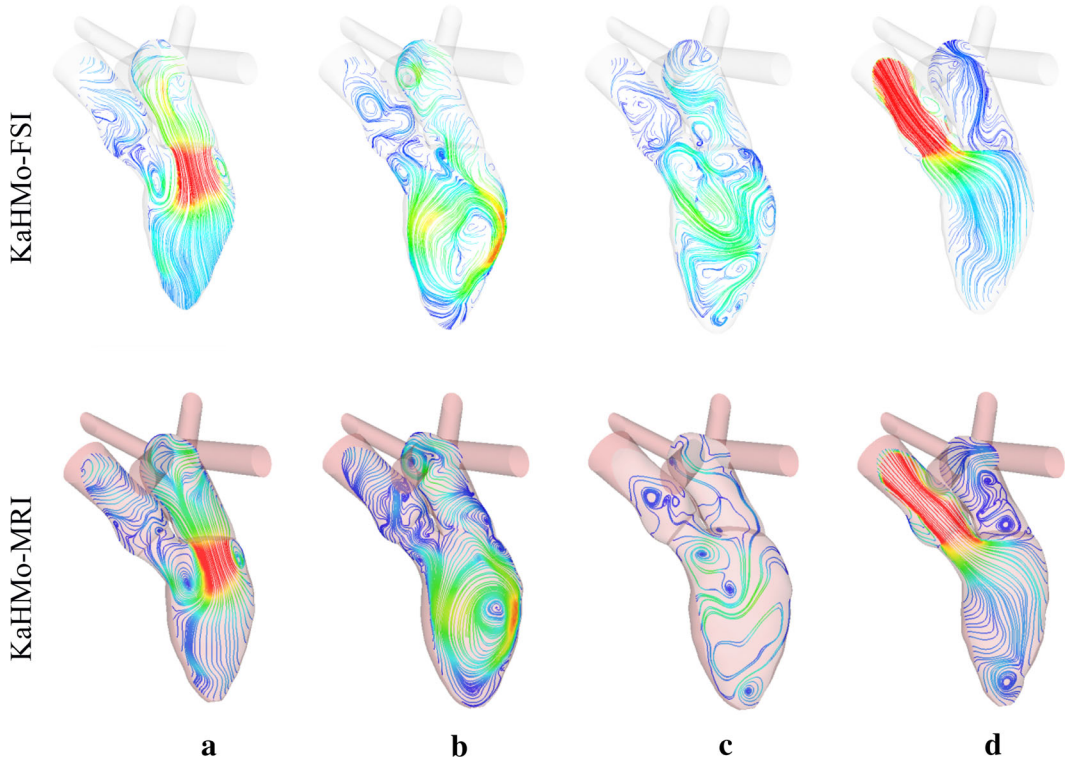

FIGURE 6. Left ventricular blood flow.

flow is blocked) is due to an inexact discretization of the mitral valve area. Additionally, the low ambient pressure level and the partial opening may amplify small fluctuations in pressure. These small oscillations have a negligible effect on the overall behavior of the heart. However, pressure-driven heart valves should be used in the future, although a pressure-driven boundary condition can lead to oscillations, too. In this case, some damping must be introduced for stabilization. The damping can—physically—be regarded as inertia and stiffness of the mitral valve and muscle fibers. After the ventricle reaches its end-diastolic volume, contraction of the myocardium starts the systole (*d*). While the inner ventricular flow structure and mixing during the diastole are mainly affected by flow aspects, such as pressure difference and vortex formation, structural mechanics plays an important role for the ejection of blood. During the early systole, dissipation of vortices increases and blood is accelerated towards the aortic valve. When the inner ventricular pressure reaches atrial pressure, the mitral valve closes and the heart continues with iso-volumetric contraction, which means that pressure increases, while the volume remains constant (see Fig. 5). When the pressure in the left ventricle exceeds aortic pressure, the aortic valve opens and ejection begins. Detailed analysis of cardiac blood flow can be found in previous publications.[25,27] The calculated blood flow in Fig. 6 shows that KaHMo-FSI is able to capture characteristic phenomena of cardiac blood flow.

DISCUSSION

In this paper we presented a patient-specific fluid–structure interaction model of left ventricular blood flow based on the ALE formulation. This advancement is part of the KaHMo and, hence, referred to as KaHMo-FSI.[16,18] The newly implemented structural model of the myocardium considers the orthotropic behavior of the human heart by using a local coordinate system and is consistent with *in vitro* studies reported in literature. The strain energy function by Holzapfel *et al.*[12] for passive behavior was partly recalibrated and newly modified to account for active contraction. One advantage of the proposed modification is the reduced computational expenditure. The simulation of six heart beats takes approx. 640 h. The fluid mechanics model accounts for non-Newtonian fluid properties and the influence of pressure boundary conditions on the circulatory system. The simulation was compared to clinical data (volume), simulations with a given motion of the endocardium (KaHMo-MRI), and literature (stresses). KaHMo-FSI is able to capture the measured volume change during one heart cycle and is in good agreement with KaHMo-MRI in

terms of quantitative and fluid flow aspects. The myocardial stresses cannot be quantified (*in vivo*) due to a lack of experimental data, but they are qualitatively reasonable for the systole and diastole compared to literature (*in vitro*). In contrast to a simulation with a given wall motion, fluid–structure interaction additionally allows for the prediction of the success of surgery, as it captures the heart function in a physically more accurate way.

The novelty of this paper is—besides the model enhancements—the introduction of a new characteristic to assess the state of health considering myocardium and blood flow.

However, some other important mechanisms have not yet been included, such as the Frank-Starling mechanism, softening of scars due heart surgery, simulation of atrial contraction, and motion of the valve plane to support filling and ejection. To assess the overall heart function the right ventricle should also be included.[38]

Another interesting aspect is that many fluid–structure interaction models of biomechanical systems (heart, vessels) often assume a load- and stress-free starting point for simulation by disregarding residual stresses. Recently, Wang *et al*. pointed out that even if residual stresses are less important to the myocardium in the diastole, a change in transmural stress distribution can be observed.[37]

CONFLICT OF INTEREST

Mark-Patrick Mühlhausen, Uwe Janoske, and Herbert Oertel declare that they have no conflict of interest.

HUMAN AND ANIMAL RIGHTS AND INFORMED CONSENT

This article does not contain any studies with human or animal subjects performed by any of the authors.

REFERENCES

[1]de Vecchi, A., D. A. Nordsletten, R. Razavi, G. Greil, and N. P. Smith. Patient specific fluid-structure ventricular modelling for integrated cardiac care. *Med. Biol. Eng. Comput*. 51(11):1261–1270, 2013.

[2]Demirdzic, I., and M. Peric. Space conservation law in finite volume calculations of fluid flow. *Int. J. Numer. Methods Fluids* 8(9):1037–1050, 1988.

[3]Demirdzic, I., and M. Peric. Finite volume method for prediction of fluid flow in arbitrarily shaped domains with moving boundaries. *Int. J. Numer. Methods Fluids* 10(7): 771–790, 1990.

[4]Dokos, S., B. H. Smaill, A. A. Young, and I. J. LeGrice. Shear properties of passive ventricular myocardium. *Am. J. Physiol. Heart Circ. Physiol*. 283:H2650–H2659, 2002.

[5]Formaggia, L., A. Quarteroni, and A. Veneziani. Cardiovascular mathematics. Berlin: Springer, 2009.

[6]Fraunhofer Institute for Algorithms and Scientific Computing (SCAI). MpCCI 4.3 Documentation, 2014. (http://www.mpcci.de/fileadmin/mpcci/download/MpCCI-4.3.0/doc/pdf/MpCCIdoc.pdf).

[7]Fung, Y. C. Mathematical representation of the mechanical properties of the heart muscle. *J. Biomech*. 3:381–404, 1970.

[8]Fung, Y. C. Biomechanics—Mechanical Properties of Living Tissues (2nd ed.). New York: Springer, 1993.

[9]Fung, Y. C. Biomechanics—Circulation (2nd ed.). New York: Springer, 1997.

[10]Göktepe, S., S. N. S. Acharya, J. Wong, and E. Kuhl. Computational modeling of passive myocardium. *Int. J. Numer. Methods Biomech. Eng*. 27:1–12, 2011.

[11]Guccione, J. M., G. S. Kassab, and M. B. Ratcliffe (eds.). Computational Cardiovascular Mechanics—Modeling and Applications in Heart Failure. Berlin: Springer, 2010.

[12]Holzapfel, G. A., and R. W. Ogden. Constitutive modelling of passive myocardium: a structurally based framework for material characterization. *Philos. Trans. R. Soc. Lond. Ser. A* 367:3445–3475, 2009.

[13]Humphrey, J. D., and F. C. Yin. A new constitutive formulation for characterizing the mechanical behavior of soft tissues. *Biophys. J*. 52(4):563–570, 1987.

[14]Hunter, P. J., A. D. McCulloch, P. M. Nielsen, and B. H. Smaill. A finite element model of passive ventricular mechanics. In: Computational Methods in Bioengineering, edited by R. L. Spilker, and B. R. Simon. New York: ASME, 1988.

[15]Jones, T. N., and D. N. Metaxas. Patient-specific analysis of left ventricular blood flow. In: Medical Image Computing and Computer-Assisted Intervention—MICCAI98, Vol. 1496, edited by W. Wells, A. Colchester, and S. Delp. Lecture Notes in Computer Science, Berlin: Springer, 1998, pp. 156–166.

[16]Krittian, S. Modellierung der kardialen Strömung-Struktur-Wechselwirkung: Implicit coupling for KaHMo FSI. PhD thesis, Universiät Karlsruhe (TH), 2009.

[17]Krittian, S., U. Janoske, H. Oertel, and T. Böhlke. Partitioned fluid–solid coupling for cardiovascular blood flow: left-ventricular fluid mechanics. *Ann. Biomed. Eng*. 38(4): 1426–1441, 2010.

[18]Krittian, S., T. Schenkel, U. Janoske, and H. Oertel. Partitioned fluid-solid coupling for cardiovascular blood flow: validation study of pressure-driven fluid-domain deformation. *Ann. Biomed. Eng*. 38(8):2676–2689, 2010.

[19]LeGrice, I. J., B. H. Smaill, L. Z. Chai, S. G. Edgar, J. B. Gavin, and P. J. Hunter. Laminar structure of the heart: ventricular myocyte arrangement and connective tissue architecture in the dog. *Am. J. Physiol*. 269:H571–H582, 1995.

[20]LeGrice, I. J., P. J. Hunter, and B. H. Smaill. Laminar structure of the heart: a mathematical model. *Am. J. Physiol. Heart Circ. Physiol*. 272:H2466–H2476, 1997.

[21]Liepsch, D., G. Thurston, and M. Lee. Viscometric studies simulating blood-like fluids and their applications in models of arterial branches. *Biorheology* 28:39–52, 1991.

[22]Mühlhausen, M.-P. Strömung-struktur-gekoppelte Modellierung und Simulation des menschlichen Herzens. PhD thesis, Karlsruher Institut für Technologie (KIT), 2012.
[23]Nordsletten, D. A., S. A. Niederer, M. P. Nash, P. J. Hunter, and N. P. Smith. Coupling multi-physics models to cardiac mechanics. *Progr. Biophys. Mol. Biol.* 2009.
[24]Nordsletten, D. A., M. McCormick, P. J. Kilner, P. J. Hunter, D. Kay, and N. P. Smith. Fluid-solid coupling for the investigation of diastolic and systolic human left ventricular function. *Int. J. Numer. Methods Biomed. Eng.* 27:1017–1039, 2011.
[25]Oertel, H. (ed.). Prandtl—Essentials of Fluid Mechanics (3rd ed.). New York: Springer Science + Business Media, 2010.
[26]Oertel, H., and S. Krittian. Modelling the Human Cardiac Fluid Mechanics (4th ed.). Karlsruhe: KIT Scientific Publishing, 2012.
[27]Oertel, H., S. Krittian, and K. Spiegel. Modelling the Human Cardiac Fluid Mechanics (3rd ed.). Karlsruhe: Universitätsverlag Karlsruhe, 2009.
[28]Pedrizzetti, G., and K. Perktold. Cardiovascular Fluid Mechanics. Number 446 in CISM International Centre for Mechanical Sciences. Wien: Springer, 2003.
[29]Perschall, M. Numerische Untersuchung des Wellenpumpenkonzeptes und der mechanischen Herzunterstützung. PhD thesis, Karlsruher Institut für Technologie (KIT), 2010. (http://digbib.ubka.uni-karlsruhe.de/volltexte/1000016087).
[30]Peskin, C. S. Flow patterns around heart valves: a numerical method. *J. Comput. Phys.* 10:252–271, 1972.
[31]M. Reik. Simulation der Strömungsstruktur im menschlichen Herzen. PhD thesis, Universität Karlsruhe (TH), 2007.
[32]Schenkel, T., M. Malve, M. Reik, M. Markl, B. Jung, and H. Oertel. Mri-based cfd analysis of flow in a human left ventricle: methodology and application to a healthy heart. *Ann. Biomed. Eng.* 37:503–515, 2009.
[33]Spiegel, K. Strömungsmechanischer Beitrag zur Planung von Herzoperationen. PhD thesis, Universität Karlsruhe (TH), 2009.
[34]Streeter, D. D., and D. L. Bassett. An engineering analysis of myocardial fiber orientation in pig's left ventricle in systole. *Anat. Record* 155:503–511, 1966.
[35]Streeter, D. D., H. M. Spotnitz, D. P. Patel, J. Ross, and E. H. Sonnenblick. Fiber orientation in the canine left ventricle during diastole and systole. *Circ. Res.* 24:339–347, 1969.
[36]Tay, W. B., Y. H. Tseng, L. Y. Lin, and W. Y. Tseng. Towards patient-specific cardiovascular modeling system using the immersed boundary technique. *BioMed. Eng. OnLine* 10:52, 2011.
[37]Wang, H. M., X. Y. Luo, H. Gao, R. W. Ogden, B. E. Griffith, C. Berry, and T. J. Wang. A modified Holzapfel-Ogden law for a residually stressed finite strain model of the human left ventricle in diastole. *Biomech Model Mechanobiol* 13(1):99–113, 2014.
[38]Watanabe, H., S. Sugiura, and T. Hisada. The looped heart does not save energy by maintaining the momentum of blood flowing in the ventricle. *Am. J. Physiol. Heart Circ. Physiol.* 294:H2191–H2196, 2008.